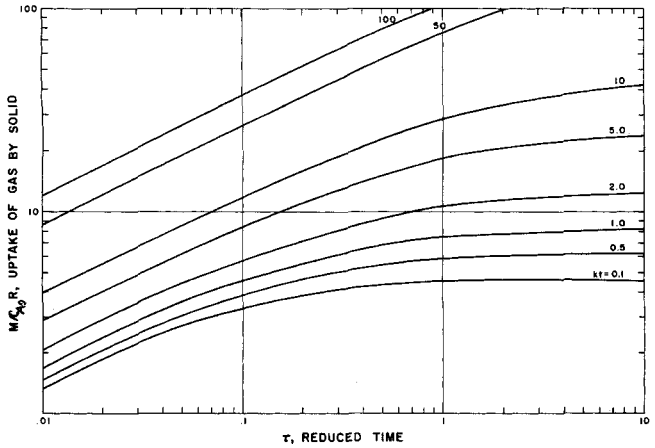

Fig. 2. Uptake of gas in a solid sphere as a function of time, with diffusion and kinetics influencing reaction rate.

on this plot would be parallel, with the slope being ½.

When the intrinsic diffusion and reaction rates are of comparable magnitude, we have a pseudo first-order reaction, and the concentration of A is described by

$$\frac{\partial C_A}{\partial t} = \frac{1}{r^2}\frac{\partial}{\partial r}(r^2 C_A) - kt \qquad (11)$$

if we assume the gas concentration is constant at the sphere surface. The solution of Equation (11) is easily obtained from results derived by Danckwerts (*4*); the uptake per particle of gaseous A is

$$M = 8\pi \frac{DC_{A0}}{R} \sum_{n=1}^{\infty} \left\{ \frac{kt}{k + Dn^2\pi^2/R^2} + \frac{Dn^2\pi^2/R^2}{(k + Dn^2\pi^2/R^2)^2}\left[1 - \exp(-t(k + Dn^2\pi^2/R^2))\right] \right\} \qquad (12)$$

or

$$\frac{M}{C_{A0}R} = 8\pi \sum_{n=1}^{\infty} \left\{ \frac{\tau(kt)}{kt + n^2\pi^2\tau} + \frac{n^2\pi^2\tau}{(kt + n^2\pi^2\tau)^2}\left[1 - \exp(-kt - n^2\pi^2\tau)\right] \right\}$$

This result is shown in Figure 2.

When the spheres are of different sizes, the uptake of gas must be summed over all particles. If the size distribution is logarithmiconormal, this summation may be achieved by employing arbitrary segments of the distribution. The process of summation in this fashion has been illustrated by Gallagher (*5*).

ACKNOWLEDGMENT

The Burroughs B5500 computer of the University of Denver has been used for calculations. Guillermo Nino assisted with graphs.

NOTATION

A^* = constant, equal to $\sqrt{4/\pi}\,/\mathrm{erf}\sqrt{\alpha/D}$
C_A = concentration of species A in solid
C_{A0} = concentration of species A in gas
C_{B0} = concentration of species B in unreacted solid phase
D = diffusion coefficient of species A in solid medium
k = reaction rate constant
M = uptake of species A by particle
r = radial coordinate in spherical particle
r' = radial position of moving boundary in spherical particle
R = radius of spherical particle
t = time
u = combined variable, equal to $C_A r$
x = linear distance coordinate in semi-infinite medium
x' = position of moving boundary in semi-infinite medium
α = constant of integration, defined by Equations (2) and (8)
ρ = radius difference, equal to $R - r$
τ = dimensionless time, Dt/R^2

LITERATURE CITED

1. Lacey, D. T., J. H. Bowen, and K. S. Basden, *Ind. Eng. Chem. Fundamentals*, **4**, 275 (1965).
2. Danckwerts, P. V., *Trans. Faraday Soc.*, **46**, 701 (1950).
3. Sherwood, T. K., and R. L. Pigford, "Absorption and Extraction," 2nd Ed., p. 335, McGraw-Hill, New York (1952).
4. Danckwerts, P. V., *Trans. Faraday Soc.*, **47**, 1014 (1951).
5. Gallagher, K. J., *Proc. Internatl. Conf. Reactivity of Solids*, 192, Munich (1964).

Flow Behavior of a Dilute Polymer Solution in Circular Tubes at Low Reynolds Numbers

NEIL S. BERMAN

Arizona State University, Tempe, Arizona

Dilute polymer solutions are of interest due to their drag reducing properties at high rates of flow. At lower flow rates in pipes these solutions exhibit apparent Newtonian behavior when pressure drop vs. flow rate data are exam-

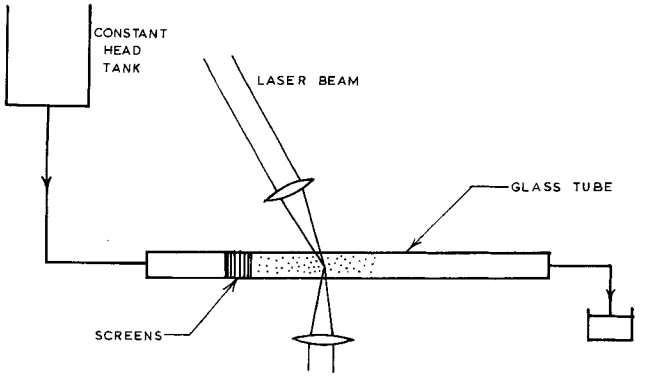

Fig. 1. Experimental apparatus.

ined (*1, 2*). Other recent measurements of pipe entrance flow show the elastic effects present in these dilute polymer solutions at moderate flow rates (*3*). Little data are available at very low velocities when elastic effects should be minimized. In this work entrance velocity profiles and fully developed velocity profiles were measured on a 100 ppm. Separan AP 30 solution (partially hydrolyzed polyacrylamide of molecular weight $1 - 3 \times 10^6$) at low flow rates. The laser Doppler measurements were made after 100 ppm. of latex particles 0.5 μ in diameter were added to aid in light scattering. The results show definite non-Newtonian behavior.

THEORY

For incompressible, isothermal flow in circular pipes, when the velocity is a function of the radial coordinate only,

$$\tau_{rz} = \frac{\Delta p}{2L} r \tag{1}$$

If in addition the fluid is Newtonian

$$\tau_{rz} = -\mu \frac{dv_z}{dr} \tag{2}$$

For other fluids this can be generalized to

$$\tau_{rz} = -\eta \frac{dv_z}{dr} \tag{3}$$

where η is a function of τ_{rz} or dv_z/dr. Some models which are simple to use and successfully fit many experimental results are the

$$\text{Power law, } \eta = \left| \frac{dv_z}{dr} \right|^{n-1} \tag{4}$$

and Ellis model,

$$\eta = \frac{\eta_o}{1 + \left| \frac{\tau_{rz}}{\tau_{1/2}} \right|^{\alpha-1}} \tag{5}$$

Many other empirical and semiempirical models have been proposed.

Near the pipe entry the velocity is a function of both the radial and axial coordinates and the rheological equation of state must be further generalized. The problem including viscoelastic effects has been recently discussed by Metzner and White (*4*).

EXPERIMENTAL PROCEDURE

The laser Doppler instrument has been described previously (*5*). Light from a small helium-neon laser is split into two beams. One is sent directly to the photocathode of a photomultiplier tube. The other is focused on a spot in the flow tube. Scattered light at an angle of approximately 10 deg. is collected by a lens and recombined with the first beam at the photomultiplier. The beat signal displayed on a spectrum analyzer is proportional to the velocity in the scattering volume. The velocities in this work were read directly from the spectrum analyzer signal displayed on an *x-y* recorder along with a frequency standard signal.

The scattering volume for the laser Doppler instrument may be approximated by

$$V_s = 18.7\ F^4\lambda^3 \tag{6}$$

where F is the lens f number of the collecting lens and λ is the wave length of the light, when the volume is a cylinder defined by the diameter of the first zero in the Airy disk diffraction pattern and the length at which the light falls in intensity by 20% (*6*). For the lens in this work, 1 in. in diameter by 5 in. focal length, the scattering volume was 3×10^{-6} cu.mm. and the cylinder length along the radius of the tube, 0.06 mm.

A schematic diagram of the apparatus is shown in Figure 1. Flow from a constant head reservoir was passed through a 4 ft. section of glass tubing, collected and weighed. An artificial entrance was created by placing a plug made of brass screens inside the glass tube. The plug consisted of 25 screens with the last screen and every third screen before it 80 mesh, and the remaining 16 screens 40 mesh. Each screen was rotated 45 deg. compared to its neighbors. The screens were punched to the exact diameter of the glass tube and inserted using an aluminum rod. The final plug was self-supporting and at right angles to the tube axis. The tube was mounted on a mill table which could be moved to change the location of the velocity measurement. The identical set up was used first with water as the fluid, as reported previously (*5*).

In addition to the laser Doppler measurements pressure drop vs. flow rate data were measured in a plastic tube 6 ft. long. The pressure taps were connected to a differential manometer using benzyl acetate as the heavy fluid. Other results were obtained with a Wells-Brookfield cone and plate microviscometer. In both cases data could not be obtained at the lowest flow rates used with the laser Doppler instrument.

The Separan solution was prepared by slowly dissolving the powder in water. Then the latex particles were added to the solution. Portions of the original solution without particles were saved for testing. Since the experimental measurements were carried out over a period of time, checks on the viscosity using a modified Stormer viscometer were made and several tests were run at the highest flow rate on the first day of experimentation and at later times. No significant changes could be found in the viscosity of the material. Even after ten months of storage no significant change, compared to a fresh solution, could be detected when the Wells-Brookfield microviscometer was used. In the tests other than those under actual flow conditions only the highest flow condition at the wall could be checked.

EXPERIMENTAL RESULTS

A typical velocity profile measured with the laser Doppler flowmeter is shown in Figure 2. At this flow rate and at all the other flow rates measured, the velocity profile could be fit to an Ellis model. However, one set of constants could not fit more than one flow rate. Table 1 shows the Ellis parameters assuming that α and η_o are the same for each flow. When $\tau_{1/2}$ is replaced by $0.735\ \tau_R^{0.7}$, the resulting modified Ellis model will fit all of the data of Table 1. When the shear stress at the wall is calculated

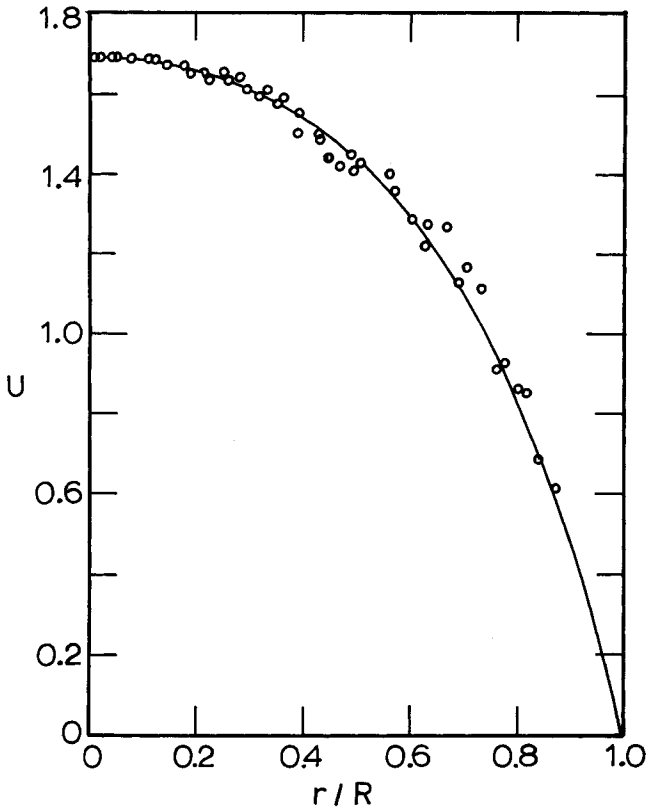

Fig. 2. Fully developed velocity profile at $\langle v_z \rangle = 2.93$ cm./sec.

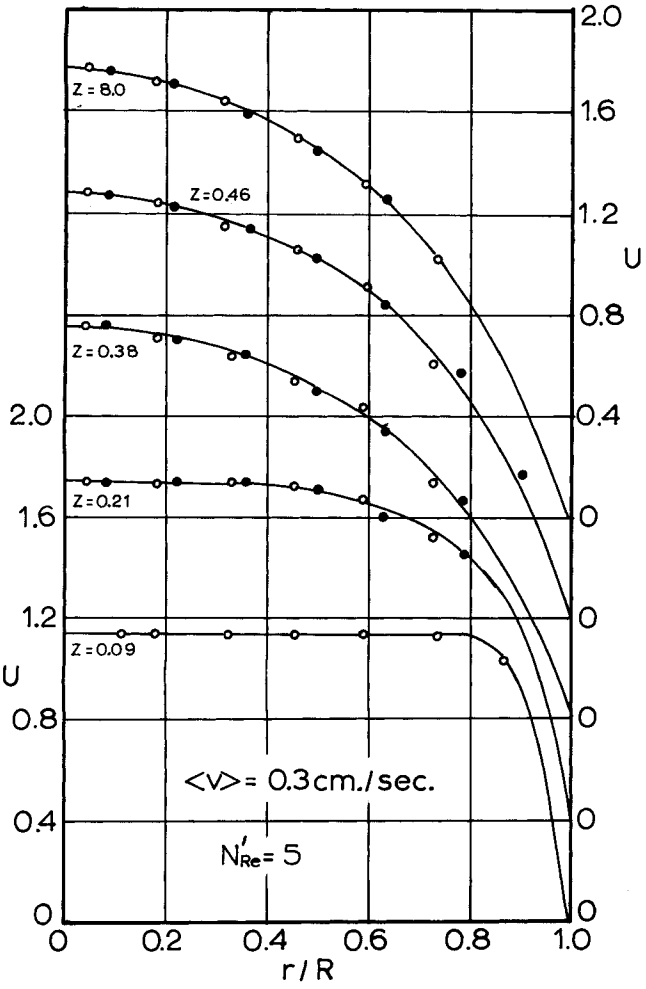

Fig. 3. Entrance profiles at lowest flow rate.

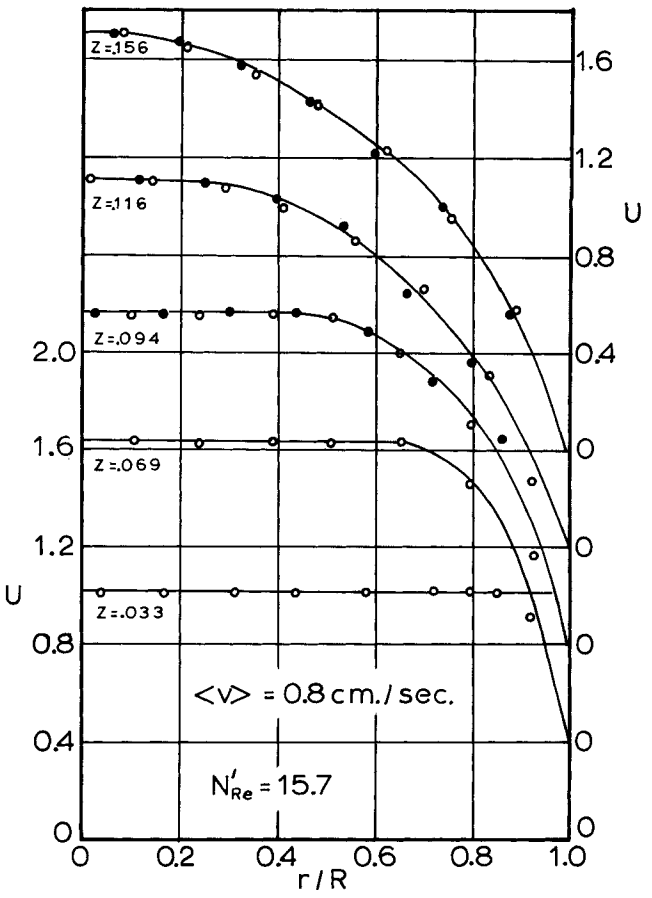

Fig. 4. Entrance profiles at intermediate flow rate.

from the model, a Reynolds number is given by

$$N'_{Re} = \frac{8\rho\langle v\rangle^2}{\tau_R} \qquad (7)$$

The Ellis model constants in Table 1 represent all of the data within ±1%. Experimentally the velocities measured at the centerline and the average velocities were within ±5% accuracy while the velocities closest to the wall

Table 1. Ellis Model Parameters For Fully Developed Flow

Measured avg. velocity cm./sec.	Measured maximum velocity cm./sec.	α	η_o, cp.	$\tau_{1/2}$ dynes / sq. cm.	N'_{Re}	Tube radius cm.
2.93	4.95	3.84	10	0.80	60.5	0.5
1.63	2.76	3.84	10	0.50	34	0.5
0.807	1.39	3.84	10	0.33	15.7	0.5
0.500	0.88	3.84	10	0.21	8.7	0.5
0.300	0.53	3.84	10	0.14	5	0.5
1.125	1.92	3.84	10	0.30	28.4	0.635
0.51	0.89	3.84	10	0.16	11.3	0.635

were of less precision. In the scattering volume at the center of the tube all velocities were approximately the same, the spectrum analyzer signal was large and narrow, giving precise results. Nearest the wall where the velocity gradient is steep, a broad low level signal represented all the velocities in the scattering volume. For the lens set up of this work, the closest approach to the wall was predicted to be 0.063 mm. from the wall after which the signal represented some fluid velocities and some reflected images in the glass tube from points much nearer the center.

Many different viscosity measurements were made in

addition to the laser Doppler flow data in an attempt to independently characterize the fluid. In the same range as the laser Doppler data direct measurements of pressure drop vs. flow rate showed a Newtonian fluid with a viscosity of 3.52 centipoise ± 3% over a shear stress range of 0.19 to 1.44 dynes/sq.cm. and shear rate up to 45.9 sec.$^{-1}$. At higher shear stress up to 5.35 dynes/cc., the solution behaved as a power law fluid with n equal to 0.73 from the cone and plate data.

Experimental velocity profiles at axial positions near the plug were measured for three different flow rates. These results are shown in Figures 3, 4, 5, and 6. Also in Figure 6, the centerline velocity development is shown for an ideal Newtonian fluid at $N_{Re} > 250$ and for water in the same tube at two comparable Reynolds numbers. Additional details on the water experiments were given in a previous paper (5).

DISCUSSION

In fully developed flow in the pipe the velocity profile of this polymer solution could be described by a power law fluid with n about 0.7 in the center of the tube and n equal to 0.9 near the wall. Although the latex particles may have affected the flow behavior, tests at higher rates of shear using a modified Stormer viscometer showed no difference with or without the latex particles.

No constitutive equation for a purely viscous fluid will account for the observed behavior at the wall over the tenfold change in flow rate. A possible explanation is that the molecules cannot travel through the tube in a random orientation near the wall when the distance to the wall is shorter than the long dimension of the molecule. Any effect of this type leading to an ordered structure near the wall would extend partially into the center of the tube as can be easily demonstrated by making higher polymer concentrations climb uphill.

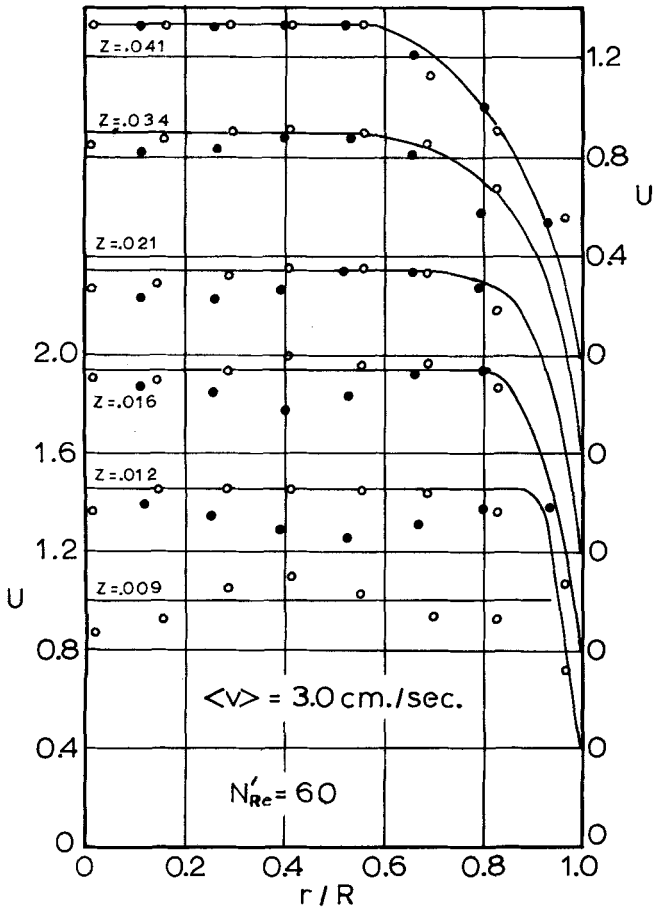

Fig. 5. Entrance profiles at highest flow rate.

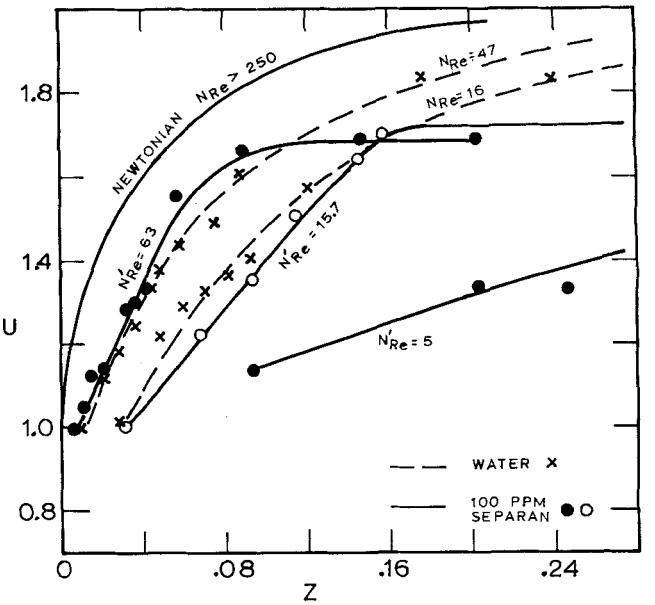

Fig. 6. Center line flow development.

In support of this discussion when a model of a power law fluid with n equal to 0.73 for the tube center is coupled with n equal to 1.0 near the wall, the transition from one n to the other occurs at 0.2 mm. from the wall. Also Figure 6 shows excellent agreement with the flow development using a Newtonian fluid at short distances from the entry. Near the entrance the flow behavior should be mostly dependent on the flow development near the wall. Note that the Newtonian data do not fall on a curve calculated by assuming a flat entrance profile and neglecting axial diffusion (shown as $N_{Re} > 200$ on Figure 6).

Beyond the immediate entry point where the wall boundary influence predominates, the velocity profile for the polymer solution develops much faster than the Newtonian comparison.

Since the Reynolds number is based on the fluid properties at the wall, this behavior is not surprising. The tube center behavior corresponds to a lower Reynolds number. A power law model with $n = 0.73$ adequately gives the entry length when compared with the entry region results of Collins and Schowalter (7) adjusted to fit the entry results in this tube for the Newtonian case. The results of Collins and Schowalter were multiplied by a factor such that the entry lengths for $n = 1$ corresponded to the data for water in this work. This factor was then used to calculate the non-Newtonian entry length.

ACKNOWLEDGMENT

The support of the University Grants Committee of Arizona State University, the Coating Committee of TAPPI, and the donors of the Petroleum Research Fund administered by the American Chemical Society is gratefully acknowledged.

NOTATION

D = tube diameter
F = f number of lens, focal length to diameter ratio
L = axial distance downstream of plug
n = power law parameter
N_{Re} = Reynolds number $D\langle v_z\rangle\rho/\mu$
N'_{Re} = Non-Newtonian Reynolds number
P = pressure
r = radial distance from center of tube
R = tube radius
v_z = axial velocity
$\langle v_z\rangle$ = average velocity

V_s = scattering volume
z = $4L/DN_{Re}$, dimensionless axial distance

Greek Letters

α = parameter in Ellis equation
λ = wave length of light
μ = Newtonian viscosity
η = generalized viscosity
η_o = parameter in Ellis equation
τ_{rz} = component of stress tensor
$\tau_{1/2}$ = parameter in Ellis equation
τ_R = wall shear stress

LITERATURE CITED

1. Hershey, H. C., and J. L. Zakin, *Ind. Eng. Chem. Fundamentals*, **6**, 381 (1967).
2. Metzner, A. B., and M. G. Park, *J. Fluid Mech.*, **20**, 291 (1964).
3. Uebler, E. A., Ph.D. thesis, Univ. Delaware, Newark (1966).
4. Metzner, A. B., and J. L. White, *AIChE J.*, **11**, 989 (1965).
5. Berman, N. S., and V. A. Santos, *ibid.*, to be published.
6. Rolfe, E., J. K. Silk, S. Booth, K. Meister, and R. M. Young, "Laser Doppler Velocity Instrument" Rept. NAS 8-20413, Raytheon Company, Sudbury, Mass. (1967).
7. Collins, M. and W. R. Schowalter, *AIChE J.*, **9**, 804 (1963).

Light Intensity Profiles in an Elliptical Photoreactor

SOLOMON M. JACOB and JOSHUA S. DRANOFF

Northwestern University, Evanston, Illinois

An interesting type of continuous flow photoreactor is one in which a tubular reactor is placed within a reflecting cavity in the form of a right cylinder with an elliptical cross section. The reactor is located with its centerline along one focus of the ellipse and a tubular light source is similarly located at the other focus. Such an assembly, which we will call an *elliptical photoreactor* for convenience, provides an excellent means for efficient irradiation of the tubular reactor and has been used extensively by recent workers.

The first use of this configuration is accredited to Baginski (*1*) who studied photoaddition of hydrogen sulfide to terminal olefins. Subsequently, it has been utilized by Gaertner and Kent (*2*) to study the photolysis of urnayl oxalate solutions, by Huff and Walker (*3*) to study the vapor phase photochlorination of chloroform, by Dolan, Dimon, and Dranoff (*4*) to study the photolysis of chloroplantinic and solutions, and by Cassano and Smith (*5*) to study vapor phase photochlorination of propane.

All of the above investigations have assumed that the light source behaves like an idealized line source emitting radiation uniformly but only in a direction normal to the source axis. This assumption of radial emission, coupled with the assumption that the surface of the elliptical chamber is a perfect reflector, leads to the conclusion that the light impinging on the reactor tube at the other focus of the ellipse will be uniform over the length of the reactor and directed radially inward. The light intensity profile over the radius of the reactor will be given by Equation (1), assuming the absorption coefficient $\mu_{\lambda,c}$ to be constant over the reactor cross section.

$$I_\lambda = \frac{S_L}{2\pi r}\left[e^{-\mu_{\lambda,c}(R-r)} + e^{-\mu_{\lambda,c}(R+r)}\right] \qquad (1)$$

This result predicts that light intensity will be a strong function of radius, becoming infinite at the reactor centerline. The last point requires that the boundary condition at $r = 0$ for a reacting system be carefully formulated (*6*).

The question to which this paper is directed is the validity of such an intensity profile in a real experimental situation. In actual practice, any tubular light source will have a finite diameter and will not behave as a true line source. Radiation from the lamp will emanate from points displaced from the lamp focus, causing the lamp to appear rather like a diffuse source. In view of the geometry of the reflector, perhaps the best one might expect in such a case is to reproduce the diffuse source at the reactor focus. In addition, imperfections in the reflecting surface will tend to diffuse the light even more. Finally, it seems obvious that any real light source will emit radiation in all directions, not merely normal to the lamp axis. This will also add to the diffuse nature of the source as well as produce a variation in light intensity in the axial direction.

In view of these considerations, it is suggested that it is much more realistic to consider the light intensity to be uniform over the radius near the reactor focus than to use a theoretical result such as Equation (1). This was

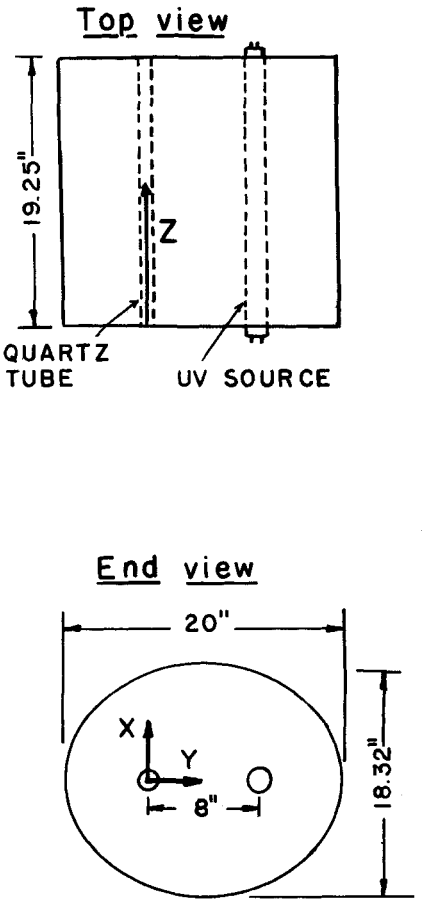

Fig. 1. Elliptical photoreactor.

Solomon M. Jacob is with Mobil Oil Co., Paulsboro, New Jersey.